

# Cellular Instabilities and Self-Acceleration of Expanding Spherical Flames

C. K. Law

*Department of Mechanical and Aerospace Engineering  
Princeton University, Princeton, NJ 08544, USA*

O. C. Kwon

*School of Mechanical Engineering  
Sungkyunkwan University, Suwon, Kyunggi-do, Korea*

## Introduction

In the present investigation we aim to provide experimental information on and thereby understanding of the generation and propagation of spark-ignited, outwardly propagating cellular flames, with three major focuses. The first is to unambiguously demonstrate the influence of the four most important parameters in inducing hydrodynamic and diffusional-thermal cellularities, namely thermal expansion, flame thickness, non-unity Lewis number, and global activation energy. The second is to investigate the critical state for the onset of cellularity for the stretch-affected, expanding flame [1-4]. The third is to identify and consequently quantify the phenomena of self-acceleration and possibly auto-turbulization of cellular flames [5, 6]. Due to space limitation the effects of activation energy and the critical state for the onset of cellularity will not be discussed herein. Details can be found in Ref. 7.

Experiments were conducted using  $C_3H_8$ -air and  $H_2$ - $O_2$ - $N_2$  mixtures for their opposite influences of nonequidiffusivity. The additional system parameters varied were the chamber pressure ( $p$ ) and the mixture composition including the equivalence ratio ( $\phi$ ). From a sequence of the flame images we can assess the propensity of cell formation, and determine the instantaneous flame radius ( $R$ ), the flame propagation rate, the global stretch rate experienced by the flame, the critical flame radius at which cells start to grow, and the average cell size.

## Effects of Instability Parameters

The hydrodynamic theory of Darrieus [8] and Landau [9] shows that, in the limit of an infinitely thin flame propagating with a constant velocity, the flame is unstable to disturbances of all wavelengths. The growth rate is proportional to the density jump across the flame, increasing with increasing  $\sigma$ . Thus  $\sigma$  is probably the most sensitive parameter controlling the onset of hydrodynamic instability.

Next to  $\sigma$ , the flame thickness  $\delta_f$  is also expected to have a strong influence on the hydrodynamic instability, for two reasons. First, it measures the influence of curvature which, being positive for the expanding flame, has a stabilizing effect on the cellular development. The thinner the flame, the weaker is the influence of curvature and consequently the stronger is the destabilizing propensity. The second influence is that it controls the intensity of the baroclinic torque developed over a slightly wrinkled flame surface, which depends on the density gradient across the flame and the pressure gradient along the flame [10]. Since the density gradient increases with decreasing flame thickness, development of the hydrodynamic instability is correspondingly enhanced due to the increased intensity of the induced baroclinic torque.

For the development of the diffusional-thermal instability, an appropriate parameter representing the effect of nonequidiffusion is the flame Lewis number,  $Le$  [11]. It is well established and understood theoretically that unstretched flames are diffusionally unstable (stable) for  $Le$ 's that are smaller (greater) than a value slightly less than unity.

The last parameter of importance, especially for the present outwardly expanding flame, is the Karlovitz number, which is the nondimensional stretch rate and is defined as  $Ka = (2/R)(dR/dt)/(s_u^o/\delta_T)$ , where  $s_u^o$  is unstretched laminar burning velocity and  $t$  is time. It was theoretically shown for the stagnation flame [12] and the expanding flame [1, 2] that the associated positive stretch tends to be stabilizing. Conceptually, cells cannot form if their growth rate is smaller than that of flame expansion. Since the expanding flame suffers the strongest stretch during the initial phase of its propagation when its radius is small, the tendency for cell development is expected to increase as the flame propagates outward. The influence of stretch also shifts the critical  $Le$ , at which the flame response reverses, to a smaller value than that of the unstretched flame.

We now present in sequence the influence of  $\delta_T$ ,  $\sigma$ , and  $Le$  on the propensity of cell development, with the comparison conducted at the same or similar Karlovitz numbers.

*Flame Thickness Effects:* Figure 1 shows the burning sequences of almost diffusionally neutral, stoichiometric propane-air flames in 2, 5, and 10 atm. The corresponding flame thicknesses are  $\delta_T = 0.17, 0.10,$  and  $0.062$  mm. The sequence at 2 atm. shows that the flame surface remains smooth, with the presence of only a large ridge throughout the observation period. At 5 atm. a few large cracks, formed as a consequence of the disturbance caused by the spark discharge, persist down to  $Ka = 0.05$ . However, when  $Ka$  is reduced to 0.03, small cells of an average size of 3.6 mm emerge. The sequence at 10 atm. shows that the cracks first grow in a self-similar manner up to  $Ka = 0.08$ . Then further cracking through branching is developed, as seen for  $Ka = 0.05$ . Eventually the average cell size is reduced to 1.1 mm at  $Ka = 0.03$ . The above flame morphology readily substantiates the concept that positive stretch and a thicker flame tend to delay the onset and development of hydrodynamic cells, and that as the flame becomes thinner not only it is destabilized earlier (i.e. for larger values of  $Ka$ ), but the cell size is also smaller.

*Thermal Expansion Effects:* Figure 2(a) shows the burning sequences of two diffusionally stable flames that have different values of  $\sigma$  but nearly the same values for other parameters: namely a  $\phi = 0.9, p = 10$  atm., propane-air flame with  $\sigma = 7.7, \delta_T = 0.068$  mm, and  $Le = 1.6$ , and a  $\phi = 3.0, p = 5$  atm., hydrogen-air flame with  $\sigma = 5.9, \delta_T = 0.059$  mm, and  $Le = 1.7$ . Since the former has a larger expansion ratio, it is more unstable, as shown.

*Nonequidiffusive Effects:* For this demonstration, we compare in Fig. 2(b) the burning sequences of two  $p = 5$  atm.,  $\sigma = 7.7$ , propane-air flames at  $\phi = 0.9$  ( $Le = 1.6, \delta_T = 0.10$  mm) and 1.5 ( $Le = 0.95, \delta_T = 0.21$  mm), such that the former is diffusionally stable while the latter unstable. Considering that the former has a smaller  $\delta_T$  and hence is hydrodynamically more unstable, the fact that the latter actually exhibits a more prominent instability pattern illustrates the powerful destabilizing influence imposed by the diffusional-thermal instability mechanism. The absence of any cells for the diffusionally stable flame, even at  $Ka = 0.10$ , and the presence of the (large) hydrodynamic cells for the diffusionally unstable flame at  $Ka = 0.32$ , possibly triggered by the diffusional-thermal instability, are particularly worth noting.

### Self-Acceleration of Cellular Flames

A series of crucial questions can be asked about the propagation rate of the expanding flame. First, after development of the cells, will the wrinkled flame propagate faster than the original smooth flame? Second, if it is faster, will it accelerate? Third, if it accelerates, will the acceleration be constant? Stated alternatively, by determining the flame radius history  $R(t) \sim t^\alpha$ ,

and hence the propagation velocity  $dR(t)/dt \sim t^{(\alpha-1)}$ , affirmative answers to the above three questions would require  $\alpha$  assuming a constant value greater than unity. Furthermore, a constant  $\alpha$  would imply that the flame propagation and morphology have a fractal character, and that if the fractal dimension is close to that of turbulent flame propagation, the self-acceleration process of the wrinkled flame propagation can be considered as one of auto-turbulization [5, 6, 13].

Figure 3 plots  $R(t)$  for three highly unstable flames of H<sub>2</sub>-15%O<sub>2</sub>-N<sub>2</sub> mixtures of  $\phi = 0.5$ , 1.0, and 1.5, at 15 atm. The corresponding  $Le$  are 0.40, 0.94, and 1.65. The data were subsequently fitted according to  $R(t) = R_o + At^\alpha$ , where  $R_o$  is the virtual origin, representing the effect of the initial period of steady propagation. The fitting yields  $R = 0.0013 + 1.90t^{1.26}$  for  $\phi = 0.5$ ;  $R = -0.0015 + 41.53t^{1.36}$  for  $\phi = 1.0$ ; and  $R = -0.0032 + 26.04t^{1.23}$  for  $\phi = 1.5$ , where  $R$  is in  $m$  and  $t$  in sec. The correlation of the data in the numerical fitting is accurate to 99.9%. The inset shows the corresponding  $R(t) - R_o$  in logarithm coordinates, demonstrating the linearity of the fitting and hence the constancy of  $\alpha$ .

The above fitting shows that all the three flames are self-accelerating. The acceleration exponents determined for the three cases are 1.26, 1.36, and 1.23, which do not show any particular pattern in relation to any of the flame parameters. Indeed, the three values are purposely shown as typical values since at the present state it is difficult to pin down a precise number, if indeed there exists a precise number. However, they are smaller than the value of 1.5 reported in Ref. [5], but are basically within the range of 1.25 to 1.5 mentioned in a subsequent publication [14]. Thus by using the relation  $\alpha = 1/(1-d)$  [6], where  $d$  is the fractal excess, our results basically yield  $d$  in the range of 0.20 to 0.25, implying a fractal dimension,  $(2+d)$ , of 2.20 to 2.25.

## Summary

From high-speed imaging of outwardly propagating propane-air and hydrogen-oxygen-nitrogen flames under elevated pressures, it was demonstrated that hydrodynamic instability is greatly enhanced with increasing pressure and hence decreasing flame thickness. The cellular flames were found to be self-accelerating, including those that are diffusionally unstable, with fractal dimensions between 2.20 and 2.25.

## References

1. Istratov, A.G., and Librovich, V.B., *Acta Astronautica* 14: 453 (1969).
2. Bechtold, J.K., and Matalon, M., *Combust. Flame* 67: 77 (1987).
3. Bradley, D., Cresswell, T.M., and Puttock, J.S., *Combust. Flame* 124: 551 (2001).
4. Kwon, O.C., and Faeth, G.M., *Combust. Flame* 124: 590 (2001).
5. Gostintsev, Yu.A., Istratov, A.G., and Shulenin, Yu.V., *Combust. Expl. Shock Waves* 24: 563 (1989).
6. Bychkov, V.V., and Liberman, M.A., *Physics Reports* 325: 115 (2000).
7. Kwon, O.C., Rozenchan, G. and Law, C.K., *Proc. Combust. Inst.*, 29, (2002), in press.
8. Darrieus, G., *La Technique Moderne* 30: 18 (1938).
9. Landau, L.D., *Acta Physicochem* 19: 77 (1944).
10. Pan, K.L., Qian, J., and Law, C.K., *Proc. Combust. Inst.*, 29, (2002), in press.
11. Sivashinsky, G.I., *Ann. Rev. Fluid Mech.* 15: 179 (1983).
12. Sivashinsky, G.I., Law, C.K., and Joulin, G., *Combust. Sci. Tech.* 28: 155 (1982).
13. Filyand, L., Sivashinsky, G.I., and Frankel, M.L., *Physica D* 72: 110 (1994).
14. Gostintsev, Yu.A., Istratov, A.G., Kidin, N.I., and Fortov, V.E., *High Temp.* 37: 282 (1999).

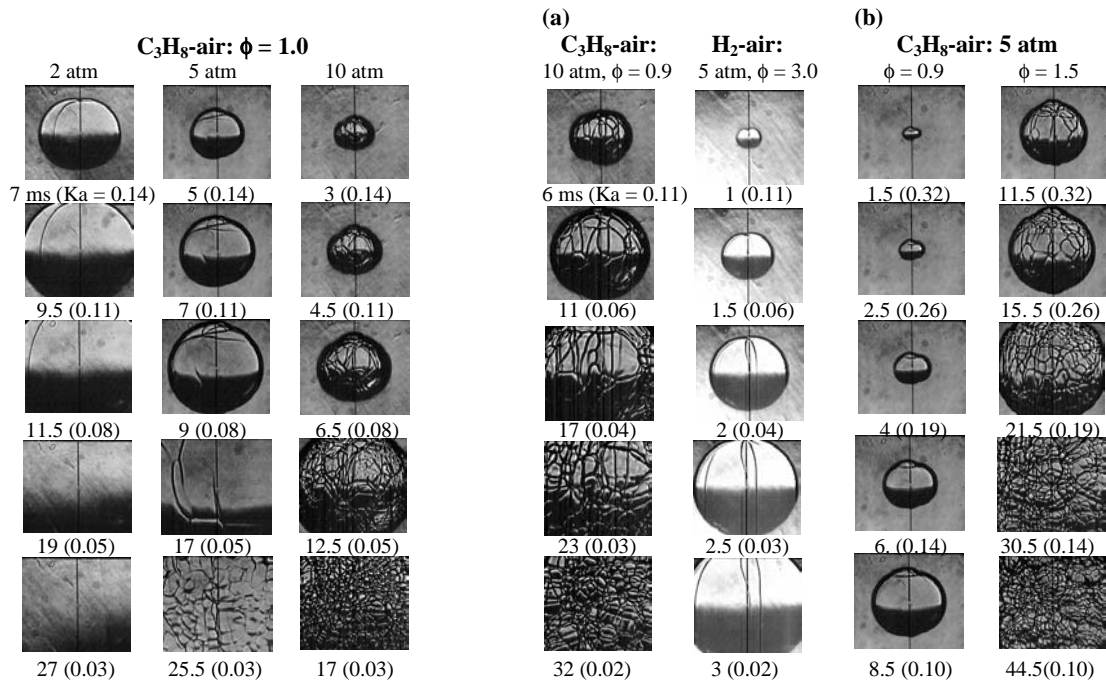


Figure 1. Schlieren photographs of stoichiometric C<sub>3</sub>H<sub>8</sub>-air flames at 2, 5, and 10 atm.

Figure 2. Schlieren photographs of (a) C<sub>3</sub>H<sub>8</sub>-air flames of  $\phi = 0.9$  at 10 atm. and H<sub>2</sub>-air flames of  $\phi = 3.0$  at 5 atm., and (b) C<sub>3</sub>H<sub>8</sub>-air flames of  $\phi = 0.9$  and 1.5 at 5 atm.

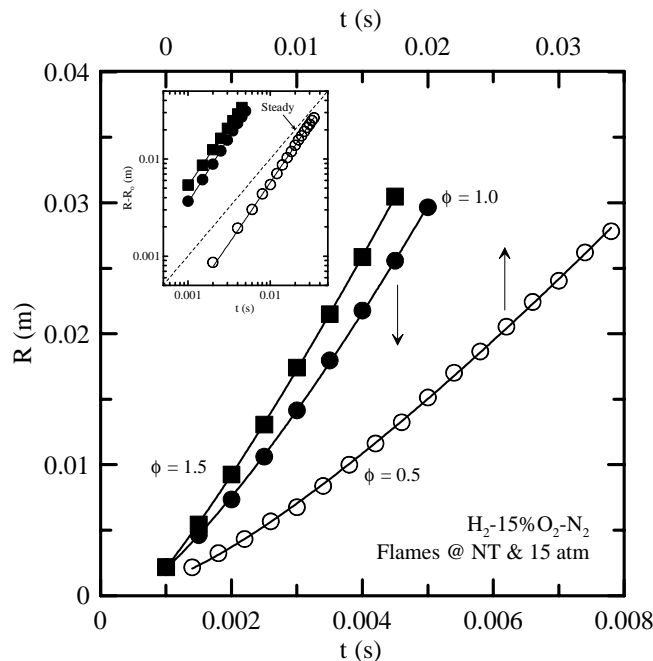


Figure 3. Flame radii as a function of time for H<sub>2</sub>-15%O<sub>2</sub>-N<sub>2</sub> flames of  $\phi = 0.5$ , 1.0, and 1.5 at 15 atm. Symbols represent experimental data, and lines represent fittings. The insert shows the corresponding flame radii subtracted by the respective virtual origins in logarithm coordinates.